THE PROTEIN SOCIETY

Characterizing antiprion compounds based on their binding properties to prion proteins: Implications as medical chaperones

Yuji O. Kamatari,[1] Yosuke Hayano,[2] Kei-ichi Yamaguchi,[2,3] Junji Hosokawa-Muto,[2] and Kazuo Kuwata[2,3,4]*

[1]Life Science Research Center, Gifu University, Gifu 501-1194, Japan

[2]Center for Emerging Infectious Diseases, Gifu University, Gifu 501-1194, Japan

[3]United Graduate School of Drug Discovery and Medical Information Sciences, Gifu University, Gifu 501-1194, Japan

[4]CREST, Japan

Received 25 June 2012; Revised 12 October 2012; Accepted 15 October 2012
DOI: 10.1002/pro.2180
Published online 18 October 2012 proteinscience.org

Abstract: A variety of antiprion compounds have been reported that are effective in *ex vivo* and *in vivo* treatment experiments. However, the molecular mechanisms for most of these compounds remain unknown. Here we classified antiprion mechanisms into four categories: I, specific conformational stabilization; II, nonspecific stabilization; III, aggregation; and IV, interaction with molecules other than PrP^C. To characterize antiprion compounds based on this classification, we determined their binding affinities to PrP^C using surface plasmon resonance and their binding sites on PrP^C using NMR spectroscopy. GN8 and GJP49 bound specifically to the hot spot in PrP^C, and acted as "medical chaperones" to stabilize the native conformation. Thus, mechanisms I was predominant. In contrast, quinacrine and epigallocathechin bound to PrP^C rather nonspecifically; these may stabilize the PrP^C conformation nonspecifically including the interference with the intermolecular interaction following mechanism II. Congo red and pentosan polysulfate bound to PrP^C and caused aggregation and precipitation of PrP^C, thus reducing the effective concentration of prion protein. Thus, mechanism III was appropriate. Finally, CP-60, an edarabone derivative, did not bind to PrP^C. Thus these were classified into mechanism IV. However, their antiprion activities were not confirmed in the GT + FK system, whose details remain to be elucidated. This proposed antiprion mechanisms of diverse

Abbreviations: AEBSF, 4-(2-Aminoethyl) benzenesulfonyl fluoride hydrochloride; DMSO, dimethyl sulfoxide; DSS, 4,4-dimethyl-4-silapentane-1-sulfonic acid; EDTA, ethylenediaminetetraacetic acid; EGCG, epigallocatechin gallate; HSQC, Heteronuclear Single Quantum Coherence; IC_{50}, inhibitory concentration for 50% reduction of PrP^{Sc}; K_D, dissociation constant; PPS, pentosan polysulfate; PrP, prion protein; PrP(23–231), PrP residues 23–231; PrP(121–231), PrP residues 121–231; PrP*, the intermediate state between PrP^C and PrP^{Sc}; PrP^C, the cellular form of PrP; PrP^{Sc}, the scrapie form of PrP; SPR, surface plasmon resonance; TSEs, transmissible spongiform encephalopathies.

Additional Supporting Information may be found in the online version of this article.

Junji Hosokawa-Muto's current address is First Department of Forensic Science, National Research Institute of Police Science, 6-3-1 Kashiwanoha, Kashiwa, Chiba 277-0882, Japan.

Grant sponsors: Program for Promotion of Fundamental Studies in Health Sciences of the National Institute of Biomedical Innovation, the Molecular Imaging Project of Japan Society and Technology Agency, and Ministry of Education, Culture, Sports, Science & Technology, and the Research Committee of Prion Disease and Slow Virus Infection, Ministry of Health, Labour and Welfare, Japan.

**Correspondence to:* Kazuo Kuwata, Center for Emerging Infectious Diseases, Gifu University, 1-1 Yanagido, Gifu 501-1194, Japan. E-mail: kuwata@gifu-u.ac.jp

antiprion compounds could help to elucidate their antiprion activities and facilitate effective antiprion drug discovery.

Keywords: prion protein; anti-prion compounds; action mechanism; medical chaperones

Introduction

Transmissible spongiform encephalopathies (TSEs) are neurodegenerative diseases that include Creutzfeldt–Jakob disease, chronic wasting disease, scrapie, bovine spongiform encephalopathy, and others. Although the conversion of prion protein (PrP) from the normal cellular form (PrP^C) to the misfolded scrapie form (PrP^{Sc}), and the accumulation of PrP^{Sc} in the central nervous system are the characteristic features of these diseases,[1,2] the detailed structure of PrP^{Sc} and the details of the conversion reaction remain unknown. The occurrence of TSEs is associated with specific mutations in PrP, inoculation with infectious material, or spontaneous onset. Because there are currently no established therapies, it is important to identify compounds with therapeutic or prophylactic activity against TSEs. The purpose of this study was to understand the various mechanisms of action of previously reported antiprion compounds and obtain further insights into optimizing their antiprion activities as well as the conversion mechanism of prion proteins.

To date, no purification method for a unique PrP^{Sc} strain has been fully established;[3] thus, quantitative binding experiments for a single PrP^{Sc} conformer is not feasible. Ideal stoichiometric determinations of ligand binding akin to the oxygen–hemoglobin binding scheme[4] are rather restricted because of the limitation of quantifying PrP^{Sc}.

In contrast, populations of PrP^{Sc} are considered to be kinetically regulated.[5] If the reaction rate of the $PrP^C \rightarrow PrP^{Sc}$ conversion could be successfully reduced to a certain level, the population of available PrP^{Sc} would gradually be reduced.[6] Following this strategy, we can completely examine the binding properties of ligands with PrP^C and evaluate their stabilization effects on PrP^C, their interference effects on the interaction between PrP^C and PrP^{Sc}, and such other effects. These activities are well represented by the notion of chemical chaperones.[6]

We previously reported a variety of antiprion compounds that were discovered based on the structures and dynamics of prion proteins.[6,7] Among these antiprion compounds, GN8[6] and its derivatives[8] are unique because of their affinities for PrP^C, their binding sites at atomic resolution, and their antiprion activities that were clarified in both *ex vivo* and *in vivo* experiments.[6,8] Other compounds have also been reported to bind to PrP^C and inhibit its pathogenic conversion.[7,9] Several groups have also reported various antiprion compounds based on *ex vivo* and/or *in vivo* experiments.[10–13] However, the details of their antiprion activities remain unknown. Thus, we attempted to characterize their antiprion mechanisms based on their binding properties to PrP^C.

Although previous studies on antiprion compounds primarily emphasized the biological effects of these compounds (IC_{50}), this study examined the various mechanisms of antiprion effects based on their binding properties to PrP^C. Thus, this study may offer new insights into the mechanisms of prion diseases. To characterize these antiprion compounds, we determined their binding affinities to PrP^C using surface plasmon resonance (SPR) and their binding sites on PrP^C using NMR spectroscopy.

We selected 13 typical antiprion compounds, including GJP49, GJP14, quinacrine, Congo red, epigallocatechin gallate (EGCG), pentosan polysulfate (PPS), CP-60, Edaravone derivative 13, D-PEN, and Indole-3-glyoxylamide derivatives (see Table I). We classified these compounds into several classes based on their binding properties to PrP^C. GJP49 and GJP14 are antiprion compounds that were discovered through *in silico* screening.[7] Quinacrine, which has been used as an antimalarial drug for over 60 years, has also been shown to be an antiprion compound.[10] Congo red, a dye used for staining amyloid fibrils, has been reported to have antiprion activity.[14] EGCG is a polyphenolic compound in tea that has been reported to have antiprion activity,[15] and PPS, which is used as a therapeutic agent for chronic cystitis, has also been reported to be an antiprion compound.[16,17] We also examined CP-60,[11] edaravone derivative 13,[18] D-PEN,[19] and indole-3-glyoxylamide derivatives.[20] In addition, we discuss a novel concept, "medical chaperone," in the context of further optimization of these previously identified antiprion compounds.

Results

GJP49 and GJP14 specifically bind to PrP^C

We previously reported the binding affinity of GJP49 for PrP^C as determined by SPR.[7] The SPR data were fit using a 1:1 binding model of equilibrium analysis, and the dissociation constant (K_D) was estimated to be 50.8 μM. To identify the interaction sites on PrP^C for GJP49, we measured the ^1H-^{15}N HSQC spectra with or without GJP49 and superimposed them, as shown in Figure 1(A). We also calculated the chemical shift perturbations ($\Delta\delta$) of ^1H and ^{15}N nuclei in PrP^C upon binding with this compound [Fig. 1(B)], and significantly perturbed

Table I. *Antiprion Compounds Used in This Study*

Compound	Chemical structure	M.W.	Relative PrP^{Sc} level[a] (%)	Antiprion mechanism	References
GJP49	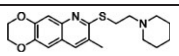	344.5	47.4	I	7
GJP14	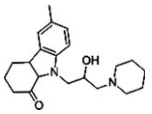	342.5	51.3	I	7
Quinacrine	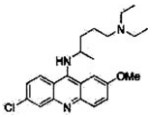	400	Toxic[b]	II	10
Congo red	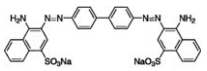	696.7	39.6	II + III	14
Epigallo-catechin gallate (EGCG)	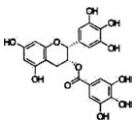	458.4	65.6	II + III	15
Pentosan polysulfate (PPS)	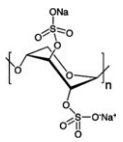	366.3n	ND[c]	II + III	16,17
CP-60	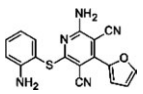	333.4	94.3	IV[d]	11
Edaravone derivative 13	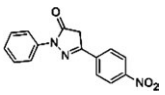	281.3	93.0	IV[d]	18
D-PEN		149.2	95.5	IV[d]	19
Indole-3-glyoxylamide derivative 2	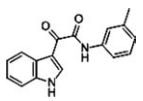	278.3	81.8	IV[d]	20
Indole-3-glyoxylamide derivative 10	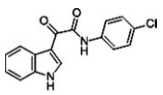	298.7	110	IV[d]	20
Indole-3-glyoxylamide derivative 12	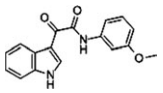	294.3	103	IV[d]	20
Indole-3-glyoxylamide derivative 13	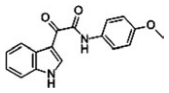	294.3	Toxic[e]	IV[d]	20

[a] Mean PrP^{Sc} level (%) using 10 μ*M* of each compound on Fukuoka-1 strain-infected GT + FK cells.
[b] Relative PrP^{Sc} level is 37.1 at 2 μ*M* for quinacrine.
[c] Though PrP^{Sc} level at 10 μ*M* cannot determined because the compound concentration could not be determined, relative PrP^{Sc} level at 10 μg/mL is 24.4 for PPS.
[d] Binding to PrP^{C} nor antiprion activities in GT + FK system were not confirmed.
[e] Relative PrP^{Sc} level is 144 at 5 μ*M* for indole-3-glyoxylamide derivative 13.

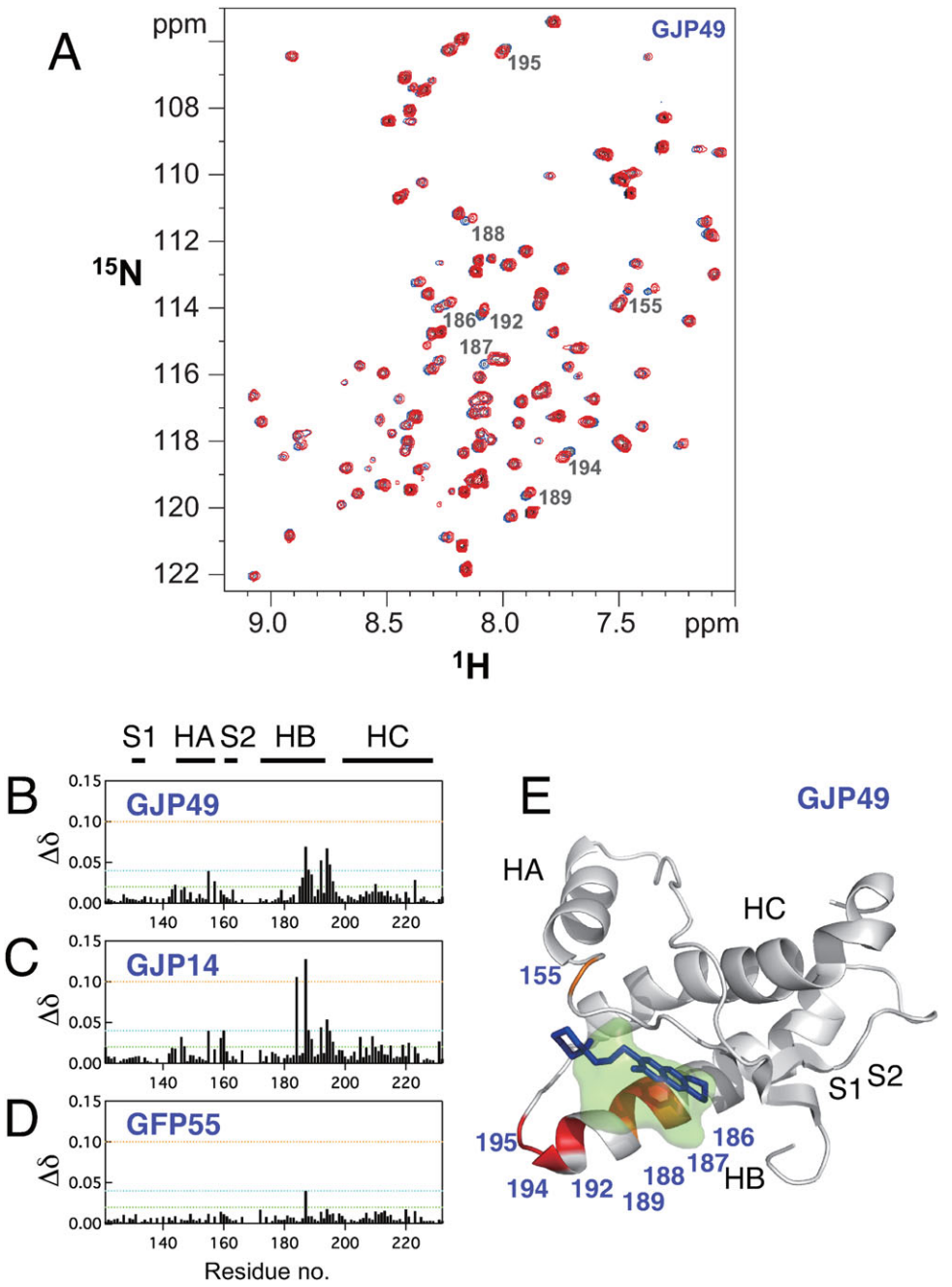

Figure 1. Characteristics of the binding sites for the antiprion compound GJP49. GJP49 was discovered by *in silico* screening using Autodock.[7] (A) ^{1}H-^{15}N HSQC spectra of ^{15}N-labeled recombinant prion protein, mouse PrP(121–231) (33 μ*M*), with (red) or without (blue) GJP49 (500 μ*M*). (B–D) Plots of chemical shift perturbations ($\Delta\delta = [(\Delta\delta_{1H})^2 + 0.17(\Delta\delta_{15N})^2]^{1/2}$) as a function of the residue number. (E) Mapping of the significantly perturbed residues on the three-dimensional structure of the prion (1AG2). The perturbed residues with $\Delta\delta$ values of >0.04 ppm are shown in red, and those with $0.4 < \Delta\delta < 0.3$ ppm are shown in orange. The binding pocket is overlaid in green. S1, HA, S2, HB, and HC indicate S1 strand, helix A, S2 strand, helix B, and helix C, respectively. The image was created using PyMol.

PrP^C residues were mapped onto the three dimensional structure of mouse PrP (PDB ID: 1AG2). Figure 1(E) shows the specific binding of GJP49 to the C-terminal region of helix B and at part of the B-C loop of PrP^C.

We also examined the interaction sites for GJP14, another effective antiprion compound that was found by *in silico* screening.[7] This compound also bound to the same region of PrP^C [Fig. 1(C)]. The region of PrP^C that binds GJP49 and GJP14 corresponds to that of GN8, another antiprion compound that we examined in a previous article.[6] This region of PrP^C undergoes a global fluctuation on a time scale of micro- to milliseconds.[21]

As a negative control for these binding experiments, we also examined the interaction sites of

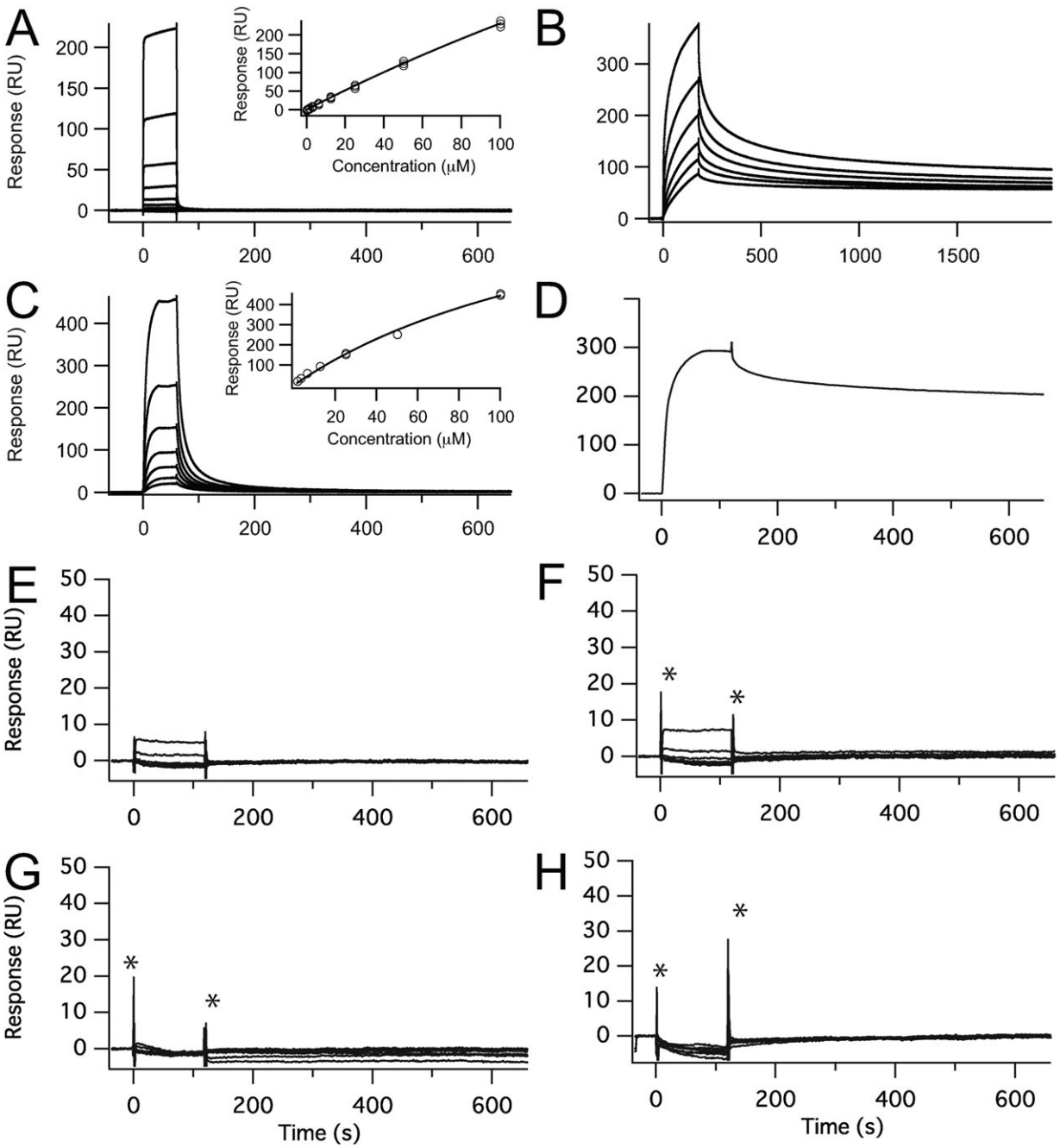

Figure 2. Surface plasmon resonance sensorgrams for various antiprion compounds. (A) Quinacrine; the concentrations from bottom to top are: 0.781, 1.56, 3.13, 6.25, 12.5, 25, 50, and 100 μ*M*. (B) Epigallocathechin gallate; the concentrations from bottom to top are: 3.91 7.81, 15.6, 31.3, 62.5, and 125 μ*M*. (C) Congo red; the concentrations from bottom to top are: 1.56, 3.13, 6.25, 12.5, 25, 50, and 100 μ*M*. (D) Pentosan polysulfate; the concentrations is: 1.95 μg/mL. (E–H) CP60, Edarabone derivative 13, D-PEN, and indole-3-glyoxylamide derivative 10; the concentrations from bottom to top are: 0.75, 1.25, 2.5, 5.0, 10, 20, and 40 μ*M*. The symbol * indicates spike noise. Insets show the compound concentration dependence of the Biacore response. For quinacrine, Congo red, and pentosan polysulfate binding experiments, recombinant mouse PrP(121–231) was fixed on the surface of the sensor chip. For epigallocatechin gallate, CP60, edarabone derivative 13, D-PEN, and indole-3-glyoxylamide derivative 10 binding experiments, recombinant mouse PrP(23–231) was fixed on the surface of the sensor chip.

GFP55, which belongs to a low-binding, ineffective group of compounds.[7] In contrast to GJP49 and GJP14, the addition of GFP55 did not result in a significant chemical shift change [Fig. 1(D)]. Therefore, we considered that GJP49 and GJP14 specifically bound to a flexible pocket of PrP^{C} and inhibited the pathogenic conversion of PrP^{C} to PrP^{Sc}.

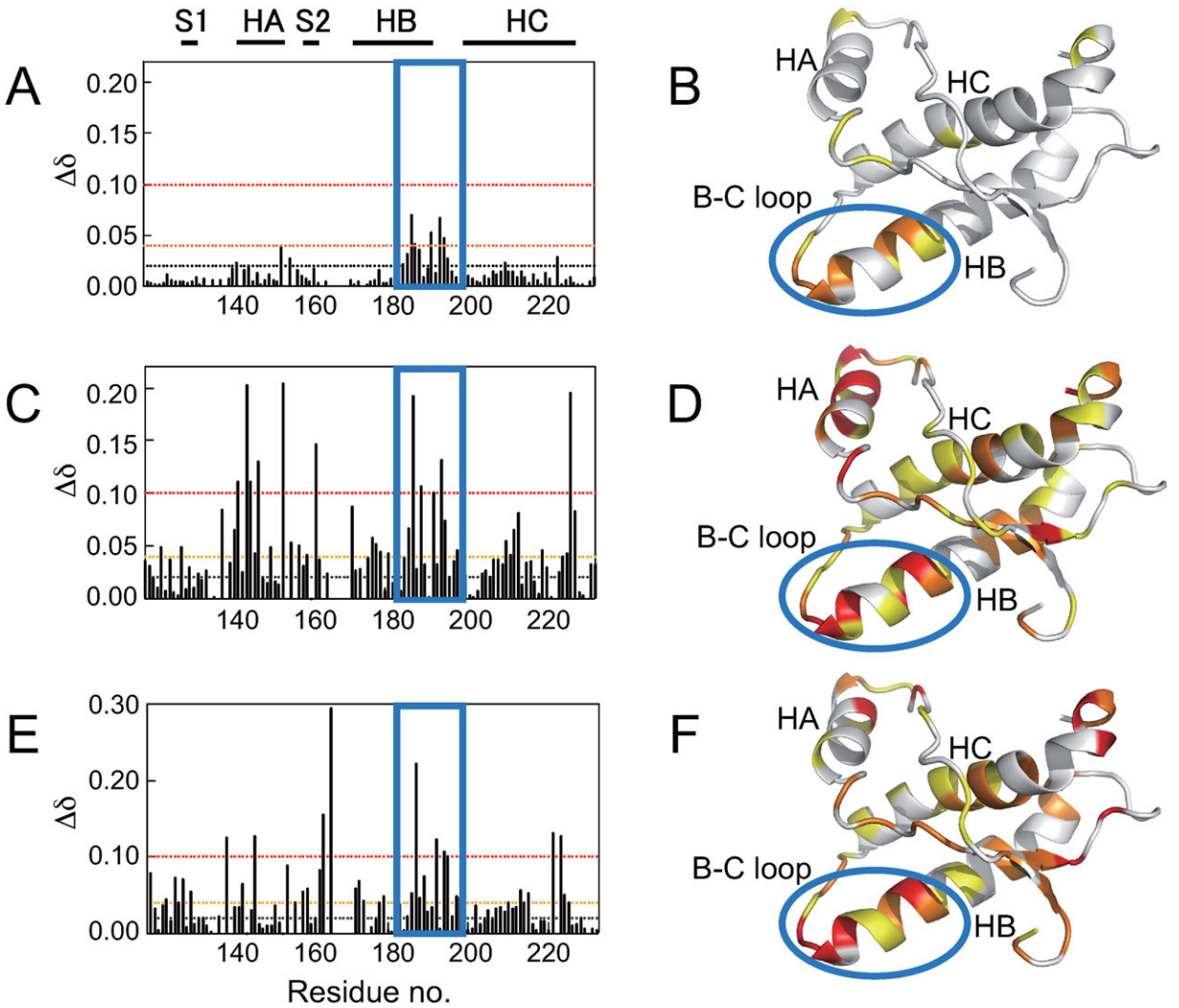

Figure 3. Chemical shift perturbations (Δδ) as a function of residue number and the mapping of Δδ onto the three dimensional structure of recombinant mouse PrP(121–231) (PDB ID: 1AG2). (A, B) GJP49, (C, D) quinacrine, and (E, F) epigallocatechin gallate (EGCG). Final concentrations of the protein and compounds were, respectively, 31 μ*M* and 500 μ*M* for GJP49 and EGCG binding experiments and 32 μ*M* and 5.3 m*M* for quinacrine binding experiment.

Quinacrine binds to PrP^C in a nonspecific manner

We analyzed SPR responses to examine the specificity of the interaction between quinacrine and PrP^C [Fig. 2(A)]. The SPR response increased as the concentration of test compound increased, without any trend toward saturation [inset in Fig. 2(A)]. The SPR response for quinacrine could not be fit using a simple binding model, which suggested nonspecific adhesion possibly due to strong hydrophobic interactions.

It has been reported that quinacrine accumulates in the brain after long-term administration.[22] In addition to PrP^C binding, quinacrine may also bind to other proteins without being degraded, which would cause the observed accumulation in the brain and significant side effects. To characterize the interaction sites between quinacrine and PrP^C, we obtained the chemical shift perturbations (Δδ) from the ^{1}H-^{15}N HSQC spectra [Fig. 3(C)] and mapped these onto the three dimensional structure [Fig. 3(D)]. When quinacrine was added to a 30.6 μ*M* solution of PrP^C at a final concentration of 500 μ*M*, no significant change in chemical shift was observed. When we increased the concentration of quinacrine (to 5.3 m*M*), the chemical shift perturbations increased to >0.04 for residues covering the entire molecular surface, particularly around parts of helices A, B, and C, including residues Y225, Y226, and D227. This result strongly suggested a nonspecific interaction.

Based on the results of an *ex vivo* assay using the GT + FK cell line,[23] the IC$_{50}$ values for GN8 and quinacrine were 1.40 μ*M* and 1.11 μ*M*, respectively.[8] The mean Δδ values with GN8 at 1.0 m*M* and PrP^C at 26 μ*M* roughly corresponded to those for quinacrine at 5.3 m*M* and PrP^C at 32.4 μ*M*, respectively. Although their IC$_{50}$ values were close, quinacrine required an approximately fourfold

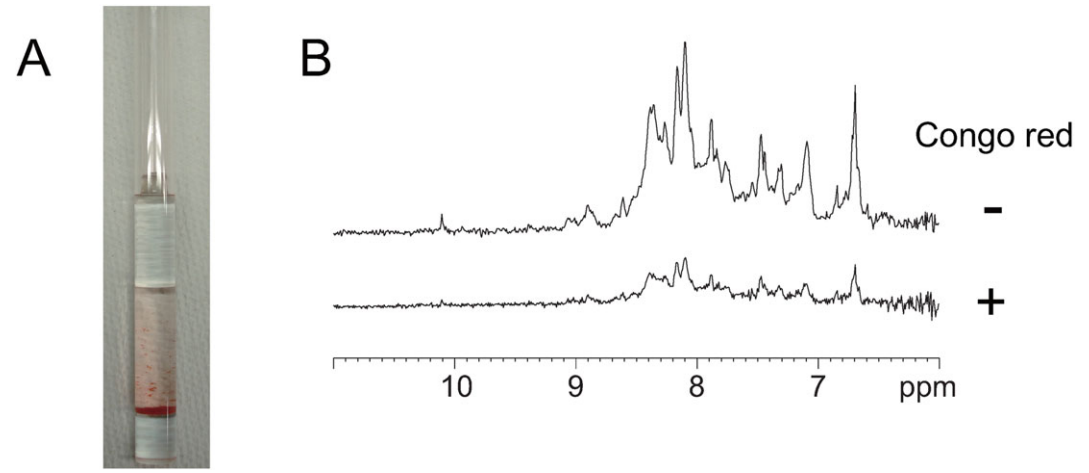

Figure 4. Aggregation and precipitation of mouse PrP(121–231) by Congo red. (A) Precipitation of mouse PrP(121–231) by Congo red in a Shigemi tube. (B) 1D ^{1}H NMR spectra with (lower trace) and without (upper trace) Congo red.

greater concentration than GN8 to reach the same $\Delta\delta$ level in its NMR spectrum.

This discrepancy can be explained by the differences in the specificities of the ligand–protein interaction (i.e., the binding regions for quinacrine are broadly distributed over the entire protein surface). In addition, the local structural stability of the ligand–protein complex may be important because structural fluctuations may reduce the $\Delta\delta$ values through an averaging effect. Quinacrine has also been reported to be transported into the intracellular space by endocytosis; lysosomes have a 10,000 times greater concentration of quinacrine than what is found in the extracellular space.[24] Thus, locally concentrated quinacrine may have been able to interact with PrP^C in the *ex vivo* experiment.

EGCG binds to PrP^C in a nonspecific manner and partially aggregates PrP^C

Although we measured the SPR responses of PrP^C upon binding with EGCG [Fig. 2(B)], the interaction was too strong to reverse the sensorgram to its original level, even after an exhaustive washing and subsequent recovery procedure. Before NMR determinations, we found that mixing PrP^C and EGCG at a molar ratio of 1:10 resulted in precipitating 80% of the PrP^C (data not shown). When we measured the ^{1}H-^{15}N HSQC spectrum for PrP^C and EGCG at a molar ratio of 1:8.2, we observed large chemical shift perturbations ($\Delta\delta$) for the regions that diffusely covered the entire molecule [Fig. 3(F)], which indicated nonspecific binding. Although EGCG binds to PrP^C, which forms aggregates and causes the precipitation of PrP^C, a significant fraction of this complex remains in the soluble phase.

Congo red promotes aggregation and reduces the concentration of PrP^C

Affinity analysis showed that increased concentrations of Congo red resulted in significantly increased SPR responses [Fig. 2(C)] without any significant saturation effect [inset in Fig. 2(C)]. Thus, Congo red nonspecifically adheres to PrP^C. In addition, PrP^C was precipitated as the concentration of Congo red was increased in the NMR tube [Fig. 4(A)]. To characterize this interaction at the atomic level, we measured the NMR spectrum for a sample of PrP^C and Congo red at a molar ratio of 1:2, but we could not observe any significant chemical shift perturbation ($\Delta\delta$; data not shown). When we increased the molar ratio of PrP^C and Congo red to 1:16.3, PrP^C was precipitated [Fig. 4(A)] and the signal heights were shifted by 20% [Fig. 4(B)].

Consequently, we could not obtain a high quality two-dimensional spectrum for the chemical shift perturbation. Thus, under *in vivo* conditions, Congo red binds nonspecifically to PrP^C and promotes its aggregation. In addition, even at a lower PrP^C concentration, this would reduce the amount of available PrP^C required for the conversion reaction. Congo red also induced aggregation of hen lysozyme and reduced the protein concentration (Supporting Information Fig. 1), indicating that the aggregation by Congo red is not specific to PrP^C.

PPS promotes aggregation and reduces the concentration of PrP^C

Affinity analysis showed that increased concentrations of PPS resulted in significantly increased SPR responses, and incomplete dissociation [Fig. 2(D)]. The amount of PPS that was bound was greater for full-length PrP, but PPS did significantly bind to the C-terminal domain of this protein (data not shown). Thus, PPS adheres strongly and nonspecifically to PrP^C. In addition, PrP^C was precipitated as the concentration of PPS was increased (data not shown), as was observed with PrP^C and Congo red. Thus, under *in vivo* conditions, PPS nonspecifically binds to PrP^C and promotes its aggregation. PPS induced

Table II. *Classification of the Antiprion Mechanisms*

Class	Mechanism	Biacore	NMR
I	Specific conformational stabilization of PrP^C	Specific binding	Specific binding
II	Nonspecific stabilization of PrP^C	Nonspecific binding	Nonspecific binding
III	Aggregation and precipitation to reduce PrP^C population	Nonspecific binding	Not detectable
IV	Interaction with molecules other than PrP^C	No binding	No interaction

aggregation of hen lysozyme and reduced the protein concentration (Supporting Information Table I), indicating that the aggregation by PPS is not specific to PrP^C.

CP-60, Edaravone derivative 13, D-PEN, and indole-3-glyoxylamide derivatives do not bind to PrP^C

The responses on the SPR sensorgrams using mouse PrP(23–231) and CP-60 [Fig. 2(E)], edaravone derivative 13 [Fig. 2(F)], D-PEN [Fig. 2(G)], indole-3-glyoxylamide derivative 10 [Fig. 2(H)], and indole-3-glyoxylamide derivatives 2, 12, and 13 (data not shown) were all minimal. Thus, these data suggested that these compounds did not directly interact with either the C- or N-terminal domain of PrP^C. As shown in Table I, CP-60, edaravone derivative 13, D-PEN, and indole-3-glyoxylamide derivatives did not inhibit PrP^{Sc} formation. The mean PrP^{Sc} levels using 10 μ*M* of each of these compounds were 94.3, 93.0, 95.5, 81.8, 110, and 103% for CP-60, edaravone derivative 13, D-PEN, and indole-3-glyoxylamide derivatives 2, 10, and 12, respectively. Indole-3-glyoxylamide derivative 13 was toxic at a concentration of 10 μ*M*. Thus we could not confirm the antiprion activities for these compounds. This could depend on the strain used for the *ex vivo* assay.

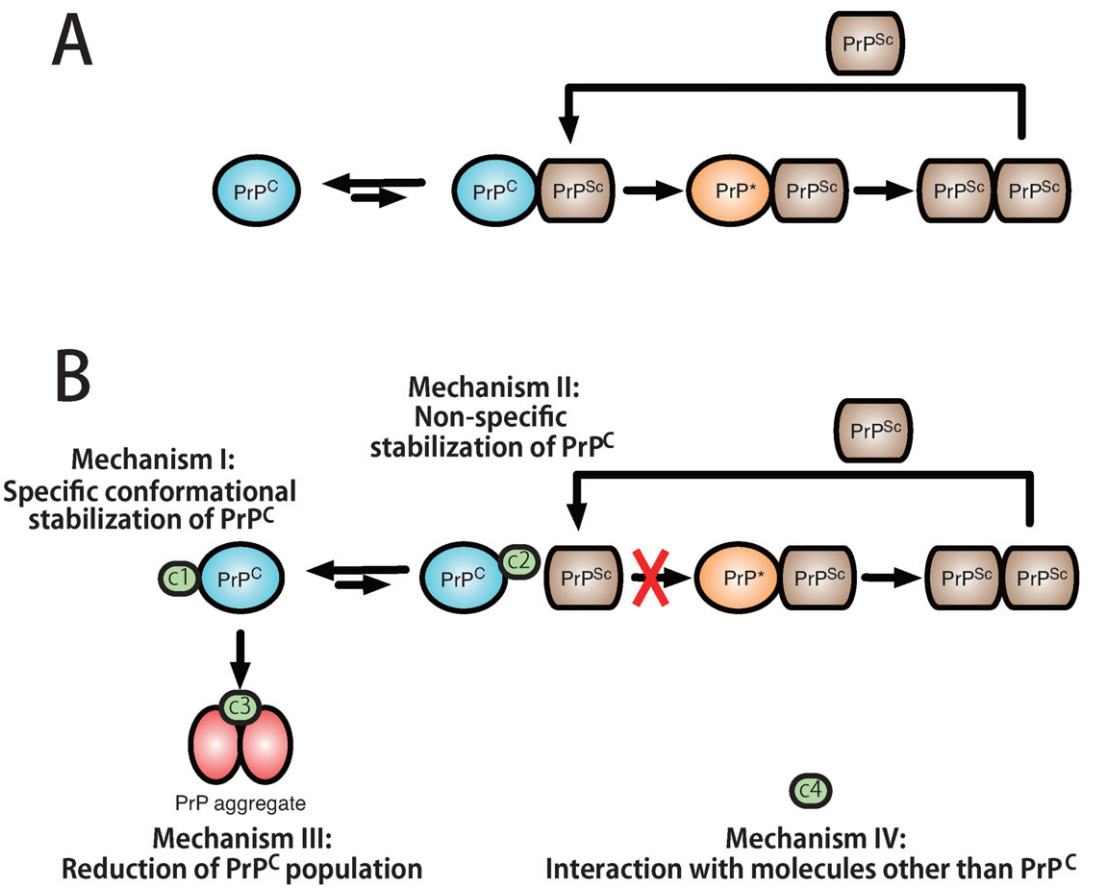

Figure 5. Illustration of the pathogenic conversion process from PrP^C to PrP^{Sc} in the absence (A) and presence (B) of antiprion compounds and the classification of antiprion mechanisms based on interactions with PrP^C. Mechanism I molecules (c1), designated "medical chaperones," stabilize the PrP^C conformation. Mechanism II molecules (c2) bind to PrP^C nonspecifically to stabilize the PrP^C and interfere with the interaction between PrP^C and PrP^{Sc}. Mechanism III molecules (c3) induce prion protein aggregation and cause precipitation, which reduces the amount of PrP^C. Mechanism IV molecules (c4) interact with molecules other than PrP^C, such as PrP^{Sc}, PrP*, or membrane proteins.

In this study, we used GT + FK cells that produce significant amounts of PrP^{res} as well as PrP^{C}. Hence the assay system using GT + FK cells is reliable, reproducible, and less sensitive to minor perturbations such as those due to the culture conditions.[9] However, it has been reported that administering these compounds to prion-infected mice days after the onset of their symptoms extended their life spans.[19] Although these compounds are reported to have antiprion activities, we could not confirm them. In other systems, they may possibly interact with the intermediate prion protein (PrP*), PrP^{Sc}, membrane proteins, or other relevant proteins,[25] and may regulate a prion's toxicity.

Discussion

Classifying antiprion mechanisms

Although there have been many reports on antiprion compounds, their mechanisms of action have not been clearly defined. In particular, comparisons of the mechanisms between various antiprion compounds are not available. Antiprion compounds can be classified as shown in Table II and Figure 5 based on their binding properties to PrP^{C}. We classified antiprion activities into four categories: I, specific conformational stabilization of PrP^{C};[6] II, nonspecific stabilization including the interference with the interaction between PrP^{C} and PrP^{Sc} as well as the contribution of binding to the hot spots; III, aggregation and precipitation to reduce the amount of available PrP^{C}; and IV, interactions with molecules other than PrP^{C}. Here, we examined the activities of representative antiprion compounds (GJP49, GJP14, quinacrine, EGCG, Congo red, PPS, CP-60, edaravone derivative 13, D-PEN, and indole-3-glyoxylamide derivatives) and characterized their antiprion activities based on their binding properties with PrP^{C}.

Characterizing antiprion compounds

GN8 and GJP49 directly bound to PrP^{C} at specific binding sites on PrP^{C} and inhibited its pathogenic conversion. These binding regions are shown in Figure 1(B,E), and are essentially the same as those for GN8 (i.e., hot spot).[6] Specific binding to this region is associated with mechanisms I.

In contrast, quinacrine and EGCG bound nonspecifically to PrP^{C} as shown in Figure 3(C,E). To check correlation between the $\Delta\delta$ values for each compound, we compared $\Delta\delta$ values for each residue between each compound (Supporting Information Fig. 2). However, except GJP14-GJP49, clear correlation could not be observed. This also indicates the nonspecific binding property of quinacrine and EGCG. This nonspecific binding may be attributed to mechanism II. For conformational stabilization, binding to the specific hot spot that is responsible for conformational instability is required, while for interference between PrP^{C} and PrP^{Sc}, nonspecific binding to PrP^{C} would be allowed to some extent because they mutually interact with large contact areas that form oligomers,[26] amyloid fibrils,[27] or nonspecific aggregates[28] depending on the characteristics of the relevant strains. Hence, small compounds can interfere with these interactions at various nonspecific sites. However, these binding regions of these compounds also included the hot spots, therefore, there may be partially attributed to mechanism I.

Congo red and PPS induced PrP^{C} aggregation and reduced its effective concentration. In general, many small compounds inhibit amyloid formation by binding with amyloidogenic proteins via π–π interactions and form aggregates.[29,30] Thus, their mechanisms of action are basically described by mechanism III. However, the nonspecific binding properties of these compounds indicate that they may also act by mechanism II, especially at low concentrations of these compounds and protein.

Finally, CP-60, Edaravone derivative 13, D-PEN, and indole-3-glyoxylamide derivatives do not bind to PrP^{C}, and we could not confirm their antiprion activities. Though in other system, they may possibly interact with other proteins or membranes and thus, indirectly reduce the amount of PrP^{Sc}. Thus, mechanism IV could be assigned.

Compounds associated with mechanism I share a common binding site

We compared the binding sites for the compounds that bound directly to PrP^{C} and found that GJP49, GJP14, quinacrine, and EGCG bound to a common site, the C-terminal region of helix B and the B-C loop, which is shown in Figure 3(A,C,E) (blue boxes) and Figure 3(B,D,F) (blue oval shapes). In a previous study, we demonstrated that GN8 also bound to this region.[6,8] This region is known to undergo global fluctuations on a time scale of micro- to milliseconds.[6] Each of the compounds examined here with antiprion activity via direct binding to PrP^{C} had affinity for this region. Thus, these compounds can be referred to as "medical chaperones" that stabilize the native conformation of the target protein and inhibit its transition to the abnormal conformation, PrP^{Sc}.

Medical chaperones can be considered to suppress the seismic fluctuations of a protein (i.e., protein quakes),[31,32] which results in destroying its native structure. Among the compounds examined in this study, GJP49 specifically bound to the common binding site. Thus, GJP49 may not induce any side effects and could be a candidate therapeutic agent for prion diseases.

It has been assumed that factor X is required for the pathogenic conversion of PrP,[25] although factor X has not yet been identified. It is reported that

quinacrine binds to Tyr225, Tyr226, and Gln227 (Asp227 for mouse)[24] which is located near the factor X" binding sites.[33] As shown in Figure 3(D), Δδ values in the presence of 2.67 m*M* quinacrine indicated that Tyr225, Tyr226, and Gln227 were also involved in the binding with quinacrine. Thus, quinacrine may inhibit the pathogenic conversion of PrP by competitive binding with factor X. However, it must be noted that even the maximum Δδ values for Tyr226 at this site were comparable to that at other quinacrine binding sites [Fig. 3(C)], and that this site was not a common binding site for the other compounds (Fig. 3).

Medical chaperones

It is considered that a high-energy barrier exists between PrP^C and PrP^{Sc},[34,35] and that prion proteins in the PrP^C state rarely overcome this barrier; they only achieve the PrP^{Sc} state when triggered by some unknown causes. Compounds in the first and second classes (GN8, GJP49, GJP14, quinacrine, and EGCG) bound to the residues surrounding the major binding pocket, which may be the cause of the seismic fluctuations that lead to pathogenic conversion. Medical chaperones prevent these protein quakes and suppress these fluctuations. Thus, these would stabilize the PrP^C conformation (i.e., reduce the free energy level of PrP^C), which would result in an increase in the energy barrier between PrP^C and PrP^{Sc}.[36] Therefore, these would suppress the pathogenic conversion of PrP^C to PrP^{Sc}.

Although the PrP^C conformations are nearly identical between species, PrP^{Sc} conformations are quite heterogeneous and are referred to as different "strains." Strain conformation is conserved after transmission between individuals.[37,38] Antiprion compounds that vary significantly in their efficiency, depending on the strain,[39] may directly affect the PrP^{Sc} conformation rather than the PrP^C conformation. A great advantage of a "medical chaperone" is that its effect is strain-independent[6,40] because it acts on PrP^C which has a common structure in nearly all mammals.

Medical chaperones also act by mechanism II, interference with the interaction between PrP^C and PrP^{Sc}, as described in the following section.

Interference with the interaction between PrP^C and PrP^{Sc} during the template-dependent self-replication process

PrP^C interacts with PrP^{Sc} during the process of pathogenic conversion. Compounds that bind to PrP^C nonspecifically can interfere with the interaction between PrP^C and PrP^{Sc}. Although there have been no evidence for the direct interference of the interaction between PrP^C and PrP^{Sc}, this mechanism constructs the critical difference from the originally proposed chemical chaperone for the misfolding diseases.[41] Specific binding of a medical chaperone with this function could be advantageous in clinical use by reducing side effects.

The possibility of administering a cocktail of antiprion compounds

We classified 13 different antiprion compounds into four classes based on their antiprion mechanisms of action. Compounds associated with different mechanisms of action can be administered together (e.g., GJP49 and indole-3-glyoxylamide derivative 13). GJP49 binds specifically to PrP^C and suppresses the available population in the intermediate state (PrP*), while indole-3-glyoxylamide derivative 13 does not bind to PrP^C, which indicates that this compound interacts with molecules other than PrP^C. Indole-3-glyoxylamide derivative 13 reduced PrP^{Sc} formation at the nanomolar concentration range when it was screened using a scrapie infected mouse cell line (SMB).[42] Cocktail administration of antiprion compounds might possibly reduce the concentration of each compound, which could decrease their associated side effects. Cocktail administration has also been reported for HIV[43,44] and yeast prions,[45] and could be useful for mammalian prion diseases.

Toward further optimization of chemical structures

GJP49, GJP14, quinacrine, and EGCG bind to the major pocket of PrP^C and contribute to its structural stabilization. We need to quantitatively evaluate the degree of stabilization using relaxation measurements for PrP^C, particularly around the major pocket in the presence of each compound. We also need to determine the structures of complexes using X-ray crystallography. This dynamical and structural information will be important for the rational optimization of antiprion compounds.

A specific interaction at the common binding site is critical for antiprion efficiency according to mechanism I. Specific interactions may also be advantageous for reducing side effects. Therefore, selecting specifically interacting derivatives may be important for compound optimization. For this purpose, we may able to use the Δδ values from NMR as shown in Figure 3. For example, quinacrine binds to PrP^C in a nonspecific manner [Figs. 2(A) and 3(C,D)] and has been reported to be toxic[22] (Table I). By selecting specifically interacting derivatives of quinacrine, we may be able to find compounds that have fewer side effects than quinacrine.

It should be noted that the above discussion was focused entirely on the interactions between compounds and PrP^C. When the interactions of compounds with PrP^{Sc} or the cell surface can be monitored, we will obtain additional insights into the

detailed mechanisms of prion diseases, which will aid in the development of therapeutics.

Conclusion

Elucidating the molecular mechanisms of action of previously identified antiprion compounds is one of the most important steps for developing novel antiprion drugs and optimizing the most promising compounds. When this strategy (i.e., "medical chaperones") has been established for prion diseases, it could also be applied to the rational design of drugs for other neurodegenerative diseases, such as Alzheimer's disease, Parkinson's disease, and amyotrophic lateral sclerosis.

Materials and Methods

Compounds

Compounds GJP49, GJP14, GJP55, and Indole-3-glyoxylamide derivatives were purchased from ASINEX (Moscow, Russia). Quinacrine, Congo red, and EGCG were purchased from Sigma-Aldrich (Japan, Tokyo). PPS, CP-60, Edaravone derivative 13, and D-PEN were obtained from bene-Arzneimittel GmbH (Munich, Germany), Ambinter (Orléans, France), Labotest (Niederschöna, Germany), and Wako Pure Chemical Industries (Osaka, Japan), respectively.

Recombinant mouse PrP

An expression plasmid for recombinant mouse PrP residues 23–231 [PrP(23–231)] was prepared according to a previously described protocol.[6] An expression plasmid for mouse PrP residues 121–231 [PrP(121–231)] was a kind gift from Professor Kurt Wüthrich and Dr. Simone Hornemann.[46] Recombinant PrP was prepared as previously described.[6] The concentrations of mouse PrP(23–231) and PrP(121–231) were estimated by absorbance at 280 nm using specific absorbances (ε_{280}) = 2.68 and 1.49 $(mg/mL)^{-1}$ cm^{-1}, respectively.

SPR measurements

Interactions between prion proteins and the different compounds were analyzed using the Biacore T200 system (GE Healthcare, Buckinghamshire, UK). Recombinant mouse PrP was immobilized on a sensor chip (CM5) according to the manufacturer's instructions. Varying concentrations of each compound were injected into the running buffer (10 m*M* HEPES buffer, pH 7.4, containing 0.15 *M* NaCl, 0.1% Surfactant P20, and 5% DMSO) for 1 to 2 min at a flow rate of 30 mL/min. Running buffer without compounds was then injected for 10 min at the same flow rate. Data were corrected by subtracting the response of blank sensor chip from that of protein-bound sensor chip, so the contribution of nonspecific binding of the compounds to SPR chip surface was removed.

Nuclear magnetic resonance (NMR) measurements and data analysis

For NMR measurements, mouse PrP(121–231) uniformly labeled with ^{15}N was prepared in 30 m*M* acetate-d_3 buffer (pH 4.5) containing 1 m*M* NaN_3, 4.5 μ*M* AEBSF, 20 μ*M* EDTA, 0.4 μ*M* Bestatin, 0.06 μ*M* pepstatin, 0.06 μ*M* E-64, and 1 n*M* DSS dissolved in 90% H_2O/10% D_2O. NMR spectra were recorded at 20.0°C on a Bruker Avance600 spectrometer (Bruker BioSpin, Rheinstetten, Germany) at Gifu University. The spectrometer operated at a ^1H frequency of 600.13 MHz and a ^{15}N frequency of 60.81 MHz. A 5-mm ^1H inverse detection probe with triple-axis gradient coils was used for all measurements. ^1H-^{15}N HSQC spectra were acquired with 2048 complex points covering 9600 Hz for ^1H and 256 complex points covering 1200 Hz for ^{15}N. NMR data were processed using the TOPSPIN software package (Bruker BioSpin, Rheinstetten, Germany) and NMR assignment and integration software Sparky.[47] Resonance frequencies in these spectra were identified using the chemical shift lists for mouse PrP(121–231).[48] The backbone ^1H and ^{15}N chemical shifts for a compound-bound protein were assigned by tracing the corresponding peaks in ^1H-^{15}N HSQC spectra determined with varying concentrations of the compounds. The protein structures were generated using PyMOL Molecular Graphics System Version 0.99rc9 (Schrödinger, LLC, NY).

Ex vivo *assay for antiprion activity*

An *ex vivo* assay was performed as described previously.[7] Briefly, we used an immortalized neuronal mouse cell line that was persistently infected with a human TSE agent (Fukuoka-1 strain),[23] which was designated GT + FK. This cell line was grown and maintained in 5% CO_2 at 37°C in D-MEM (Invitrogen, Carlsbad, CA) supplemented with 10% fetal bovine serum (Equitech-bio, Kerrville, TX), 50 U/mL penicillin G sodium, and 50 μg/mL streptomycin sulfate (Invitrogen, Carlsbad, CA). Stock solutions of the test compounds were prepared fresh in 100% DMSO at a concentration of 10 m*M* and stored at 4°C. Before use, the test compounds were diluted with medium to a concentration of 10 μ*M*. Control cells were treated with medium containing solvent alone (0.1%). Approximately 3.0×10^5 cells were plated in each well of a six-well plate, and treatment with a test compound was started 15 h later. After 72 h of treatment, cells were lysed in 150 μL of 1× Triton X-100/DOC lysis buffer.[49] Western blotting for PrP^{Sc} was done as described previously.[7]

Acknowledgments

The authors thank Professor Kurt Wüthrich and Dr. Simone Hornemann for kindly providing them with the expression plasmid for mouse PrP(121–231).

Pentosan polysulfate was kindly provided by Professor Masami Niwa and Professor Noriyuki Nishida. The authors thank Dr. Tomoharu Matsumoto, Ms. Junko Matsubara, and Ms. Miki Horii for their assistance with protein sample preparation. The authors thank Ms. Tomomi Saeki for technical help with evaluating antiprion activity.

References

1. Prusiner SB (1998) Prions. Proc Natl Acad Sci USA 95: 13363–13383.
2. Chesebro B (1999) Prion protein and the transmissible spongiform encephalopathy diseases. Neuron 24: 503–506.
3. Prusiner SB (1982) Novel proteinaceous infectious particles cause scrapie. Science 216:136–144.
4. O'Riordan JF, Goldstick TK, Ditzel J, Ernest JT (1983) Characterization of oxygen-hemoglobin equilibrium curves using nonlinear regression of the Hill equation: parameter values for normal human adults. Adv Exp Med Biol 159:435–444.
5. Harrison PM, Bamborough P, Daggett V, Prusiner SB, Cohen FE (1997) The prion folding problem. Curr Opin Struct Biol 7:53–59.
6. Kuwata K, Nishida N, Matsumoto T, Kamatari YO, Hosokawa-Muto J, Kodama K, Nakamura HK, Kimura K, Kawasaki M, Takakura Y, Shirabe S, Takata J, Kataoka Y, Katamine S (2007) Hot spots in prion protein for pathogenic conversion. Proc Natl Acad Sci USA 104:11921–11926.
7. Hosokawa-Muto J, Kamatari YO, Nakamura HK, Kuwata K (2009) Variety of antiprion compounds discovered through an in silico screen based on cellular-form prion protein structure: Correlation between antiprion activity and binding affinity. Antimicrob Agents Chemother 53:765–771.
8. Kimura T, Hosokawa-Muto J, Kamatari YO, Kuwata K (2011) Synthesis of GN8 derivatives and evaluation of their antiprion activity in TSE-infected cells. Bioorg Med Chem Lett 21:1502–1507.
9. Kimura T, Hosokawa-Muto J, Asami K, Murai T, Kuwata K (2011) Synthesis of 9-substituted 2,3,4,9-tetrahydro-1H-carbazole derivatives and evaluation of their anti-prion activity in TSE-infected cells. Eur J Med Chem 46:5675–5679.
10. Doh-Ura K, Iwaki T, Caughey B (2000) Lysosomotropic agents and cysteine protease inhibitors inhibit scrapie-associated prion protein accumulation. J Virol 74: 4894–4897.
11. Perrier V, Wallace AC, Kaneko K, Safar J, Prusiner SB, Cohen FE (2000) Mimicking dominant negative inhibition of prion replication through structure-based drug design. Proc Natl Acad Sci USA 97:6073–6078.
12. Kocisko DA, Baron GS, Rubenstein R, Chen J, Kuizon S, Caughey B (2003) New inhibitors of scrapie-associated prion protein formation in a library of 2000 drugs and natural products. J Virol 77:10288–10294.
13. Korth C, May BC, Cohen FE, Prusiner SB (2001) Acridine and phenothiazine derivatives as pharmacotherapeutics for prion disease. Proc Natl Acad Sci USA 98: 9836–9841.
14. Caughey B, Ernst D, Race RE (1993) Congo red inhibition of scrapie agent replication. J Virol 67:6270–6272.
15. Rambold AS, Miesbauer M, Olschewski D, Seidel R, Riemer C, Smale L, Brumm L, Levy M, Gazit E, Oesterhelt D, Baier M, Becker CF, Engelhard M, Winklhofer KF, Tatzelt J (2008) Green tea extracts interfere with the stress-protective activity of PrP and the formation of PrP. J Neurochem 107:218–229.
16. Doh-ura K, Ishikawa K, Murakami-Kubo I, Sasaki K, Mohri S, Race R, Iwaki T (2004) Treatment of transmissible spongiform encephalopathy by intraventricular drug infusion in animal models. J Virol 78: 4999–5006.
17. Tsuboi Y, Doh-Ura K, Yamada T (2009) Continuous intraventricular infusion of pentosan polysulfate: clinical trial against prion diseases. Neuropathology 29:632–636.
18. Kimata A, Nakagawa H, Ohyama R, Fukuuchi T, Ohta S, Doh-ura K, Suzuki T, Miyata N (2007) New series of antiprion compounds: pyrazolone derivatives have the potent activity of inhibiting protease-resistant prion protein accumulation. J Med Chem 50:5053–5056.
19. Sigurdsson EM, Brown DR, Alim MA, Scholtzova H, Carp R, Meeker HC, Prelli F, Frangione B, Wisniewski T (2003) Copper chelation delays the onset of prion disease. J Biol Chem 278:46199–46202.
20. Thompson MJ, Borsenberger V, Louth JC, Judd KE, Chen B (2009) Design, synthesis, and structure-activity relationship of indole-3-glyoxylamide libraries possessing highly potent activity in a cell line model of prion disease. J Med Chem 52:7503–7511.
21. Kuwata K, Kamatari YO, Akasaka K, James TL (2004) Slow conformational dynamics in the hamster prion protein. Biochemistry 43:4439–4446.
22. Nakajima M, Yamada T, Kusuhara T, Furukawa H, Takahashi M, Yamauchi A, Kataoka Y (2004) Results of quinacrine administration to patients with Creutzfeldt-Jakob disease. Dement Geriatr Cogn Disord 17: 158–163.
23. Milhavet O, McMahon HE, Rachidi W, Nishida N, Katamine S, Mange A, Arlotto M, Casanova D, Riondel J, Favier A, Lehmann S (2000) Prion infection impairs the cellular response to oxidative stress. Proc Natl Acad Sci USA 97:13937–13942.
24. Vogtherr M, Grimme S, Elshorst B, Jacobs DM, Fiebig K, Griesinger C, Zahn R (2003) Antimalarial drug quinacrine binds to C-terminal helix of cellular prion protein. J Med Chem 46:3563–3564.
25. Telling GC, Scott M, Mastrianni J, Gabizon R, Torchia M, Cohen FE, DeArmond SJ, Prusiner SB (1995) Prion propagation in mice expressing human and chimeric PrP transgenes implicates the interaction of cellular PrP with another protein. Cell 83:79–90.
26. Masel J, Genoud N, Aguzzi A (2005) Efficient inhibition of prion replication by PrP-Fc(2) suggests that the prion is a PrP(Sc) oligomer. J Mol Biol 345:1243–1251.
27. Wille H, Zhang GF, Baldwin MA, Cohen FE, Prusiner SB (1996) Separation of scrapie prion infectivity from PrP amyloid polymers. J Mol Biol 259:608–621.
28. Pham N, Yin S, Yu S, Wong P, Kang SC, Li C, Sy MS (2008) Normal cellular prion protein with a methionine at position 129 has a more exposed helix 1 and is more prone to aggregate. Biochem Biophys Res Commun 368:875–881.
29. Lamberto GR, Binolfi A, Orcellet ML, Bertoncini CW, Zweckstetter M, Griesinger C, Fernandez CO (2009) Structural and mechanistic basis behind the inhibitory interaction of PcTS on alpha-synuclein amyloid fibril formation. Proc Natl Acad Sci USA 106:21057–21062.
30. Nicoll AJ, Trevitt CR, Tattum MH, Risse E, Quarterman E, Ibarra AA, Wright C, Jackson GS, Sessions RB, Farrow M, Waltho JP, Clarke AR, Collinge J (2010) Pharmacological chaperone for the structured domain of human prion protein. Proc Natl Acad Sci USA 107: 17610–17615.

31. Ansari A, Berendzen J, Bowne SF, Frauenfelder H, Iben IE, Sauke TB, Shyamsunder E, Young RD (1985) Protein states and proteinquakes. Proc Natl Acad Sci USA 82:5000–5004.
32. Itoh K, Sasai M (2004) Dynamical transition and proteinquake in photoactive yellow protein. Proc Natl Acad Sci USA 101:14736–14741.
33. Cohen FE, Prusiner SB (1998) Pathologic conformations of prion proteins. Annu Rev Biochem 67:793–819.
34. Cohen FE, Pan KM, Huang Z, Baldwin M, Fletterick RJ, Prusiner SB (1994) Structural clues to prion replication. Science 264:530–531.
35. Cohen FE, Prusiner SB, Structural studies of prion proteins. In: Prusiner SB, Ed. (1999) Prion biology and diseases. New York: Cold Spring Harbor, pp191–228.
36. Yamamoto N, Kuwata K (2009) Regulating the conformation of prion protein through ligand binding. J Phys Chem B 113:12853–12856.
37. Telling GC, Parchi P, DeArmond SJ, Cortelli P, Montagna P, Gabizon R, Mastrianni J, Lugaresi E, Gambetti P, Prusiner SB (1996) Evidence for the conformation of the pathologic isoform of the prion protein enciphering and propagating prion diversity. Science 274: 2079–2082.
38. Safar J, Wille H, Itri V, Groth D, Serban H, Torchia M, Cohen FE, Prusiner SB (1998) Eight prion strains have PrP(Sc) molecules with different conformations. Nat Med 4:1157–1165.
39. Kawasaki Y, Kawagoe K, Chen CJ, Teruya K, Sakasegawa Y, Doh-ura K (2007) Orally administered amyloidophilic compound is effective in prolonging the incubation periods of animals cerebrally infected with prion diseases in a prion strain-dependent manner. J Virol 81:12889–12898.
40. Li J, Browning S, Mahal SP, Oelschlegel AM, Weissmann C (2010) Darwinian evolution of prions in cell culture. Science 327:869–872.
41. Sawkar AR, Cheng WC, Beutler E, Wong CH, Balch WE, Kelly JW (2002) Chemical chaperones increase the cellular activity of N370S beta -glucosidase: a therapeutic strategy for Gaucher disease. Proc Natl Acad Sci USA 99:15428–15433.
42. Kanu N, Imokawa Y, Drechsel DN, Williamson RA, Birkett CR, Bostock CJ, Brockes JP (2002) Transfer of scrapie prion infectivity by cell contact in culture. Curr Biol 12:523–530.
43. Montagnier L (2010) 25 years after HIV discovery: prospects for cure and vaccine. Virology 397:248–254.
44. Shafer RW, Vuitton DA (1999) Highly active antiretroviral therapy (HAART) for the treatment of infection with human immunodeficiency virus type 1. Biomed Pharmacother 53:73–86.
45. Roberts BE, Duennwald ML, Wang H, Chung C, Lopreiato NP, Sweeny EA, Knight MN, Shorter J (2009) A synergistic small-molecule combination directly eradicates diverse prion strain structures. Nat Chem Biol 5:936–946.
46. Hornemann S, Korth C, Oesch B, Riek R, Wider G, Wuthrich K, Glockshuber R (1997) Recombinant full-length murine prion protein, mPrP(23-231): purification and spectroscopic characterization. FEBS Lett 413: 277–281.
47. Goddard TD, Kneller DG (2001) SPARKY, version 3. San Francisco: University of California.
48. Riek R, Hornemann S, Wider G, Billeter M, Glockshuber R, Wuthrich K (1996) NMR structure of the mouse prion protein domain PrP(121-231). Nature 382: 180–182.
49. Nishida N, Harris DA, Vilette D, Laude H, Frobert Y, Grassi J, Casanova D, Milhavet O, Lehmann S (2000) Successful transmission of three mouse-adapted scrapie strains to murine neuroblastoma cell lines overexpressing wild-type mouse prion protein. J Virol 74:320–325.